Influence of N-Cap Mutations on the Structure and Stability of Escherichia coli HPr †

ARTICLE *in* BIOCHEMISTRY · SEPTEMBER 1996

Impact Factor: 3.02 · DOI: 10.1021/bi960349s · Source: PubMed

6 AUTHORS, INCLUDING:

Roopa Thapar
University of Texas MD Anderson Cancer Center
28 PUBLICATIONS **395** CITATIONS
SEE PROFILE

Eric M Nicholson
United States Department of Agriculture
33 PUBLICATIONS **505** CITATIONS
SEE PROFILE

Influence of N-Cap Mutations on the Structure and Stability of *Escherichia coli* HPr[†]

Roopa Thapar,[‡] Eric M. Nicholson,[§] Ponni Rajagopal,[‡] E. Bruce Waygood,[∥] J. Martin Scholtz,[§] and Rachel E. Klevit*[,‡]

Biomolecular Structure Center and Department of Biochemistry, University of Washington, Box 357742, Seattle, Washington 98195-7742, Department of Medical Biochemistry and Genetics and Department of Biochemistry and Biophysics, Texas A&M University, College Station, Texas 77843, and Department of Biochemistry, University of Saskatchewan, Saskatoon, Saskatchewan S7N 0W0, Canada

Received February 13, 1996; Revised Manuscript Received May 6, 1996[⊗]

ABSTRACT: This paper describes the effect of N-capping substitutions on the structure and stability of histidine-containing protein (HPr). We have used NMR spectroscopy and conformational stability studies to quantify changes in local and global free energy due to mutagenesis at Ser46, the N-cap for helix B in HPr. Previous NMR studies suggested that helix B of *Escherichia coli* HPr is dynamic as judged by the rate of exchange of amide protons with solvent. Ser46 was chosen because it is the site of regulatory phosphorylation in HPrs from Gram-positive bacteria, and mutation of this residue to an aspartic acid (S46D) in *E. coli* HPr (Gram-negative) also makes it a poor substrate in the bacterial phosphoenolpyruvate: sugar phosphotransferase system. Therefore, to understand the mechanism of inactivation of *E. coli* S46D HPr, as well as the effect of mutagenesis on protein stability, we have characterized three mutants of *E. coli* HPr: Ser46 has been mutated to an Asp, Asn, and Ala in S46D, S46N, and S46A HPrs, respectively. The results indicate that these N-cap replacements have a marked influence on helix B stability. The effect of mutagenesis on local stability is correlated to global unfolding of HPr. The ability of amino acids to stabilize helix B is Asp > Asn > Ser > Ala. In addition, since there are neither large-scale conformational changes nor detectable changes in the active site of S46D HPr, it is proposed that the loss of phosphotransfer activity of S46D HPr is due to unfavorable steric and/or electrostatic interactions of the Asp with enzyme I of the PTS.

During the past decade, considerable progress has been made in understanding the interactions that stabilize α-helices (Scholtz & Baldwin, 1992; Chakrabartty & Baldwin, 1995). From such studies it is clear that side chain−side chain interactions, electrostatic interactions with the helix dipole, and hydrophobic interactions within the local sequence all play key roles in the acquisition of helical structure. In alanine-based peptide models, helix formation and stability have been directly correlated to favorable side chain−main chain interactions at the helix N- and C-termini. This may be attributed to either side chain−main chain hydrogen bonding or electrostatic interaction of charged residues with the helix macrodipole, or both (Hol et al., 1978; Presta & Rose, 1988; Richardson & Richardson, 1988).

Although much is known about helix formation in isolated systems, the mechanism of helix formation in intact proteins is less well understood. The helix hypothesis predicts that (i) sequences with favorable N-caps and C-caps should be helical in globular proteins, (ii) the presence of an ionizable side chain at the helix N-terminus should affect its pK_a via charge−macrodipole interactions, and (iii) favorable N-cap substitutions should afford protection of helical amides against hydrogen exchange (Presta & Rose, 1988). Here we provide a direct test of the helix hypothesis and the hierarchical model of protein structure, focusing on a short helix within a small, globular protein.

Our model system is the histidine-containing protein (HPr) from *Escherichia coli*. HPr is a small (85−90 residues), monomeric protein with no disulfides, ligands, or prosthetic groups. The structures of a number of HPrs have been solved by crystallographic and NMR[1] techniques [reviewed in Herzberg and Klevit (1994)], and they reveal a small, globular conformation commonly referred to as an open-faced β-sandwich (Figure 1a). The key features of the structure include a four-stranded antiparallel β-sheet and three helices arranged on one face of the sheet. Two of the helices, helix A and helix C, are observed in both the X-ray and NMR structures. Helix B (Figure 1b) is observed in the

[†] This work was supported by NIH Grant RO1 DK35187 (R.E.K.), MRC of Canada Grant MT6104 (E.B.W.), and NIH Grant R29 GM52483 (J.M.S). J.M.S. is the recipient of an American Cancer Society Junior Faculty Research Award (JFRA-577), R.T. is a Merck predoctoral fellow, and E.M.N. is supported by a training grant from the NIH (T32 GM08523).

* Author to whom correspondence should be addressed. Tel: 206-543-5891. FAX: 206-543-8394. E-mail: klevit@u.washington.edu.

[‡] University of Washington.

[§] Texas A&M University.

[∥] University of Saskatchewan.

[⊗] Abstract published in *Advance ACS Abstracts,* August 1, 1996.

[1] Abbreviations: H-bond, hydrogen bond; NMR, nuclear magnetic resonance; EDTA, ethylenediaminetetraacetic acid; COSY, correlated spectroscopy; NOESY, nuclear Overhauser enhancement spectroscopy; TOCSY, total correlation spectroscopy; PE COSY, primitive exclusive COSY; HMQC, heteronuclear multiple-quantum coherence; HSQC, heteronuclear single-quantum coherence; HNHB, heteronuclear correlation of amide proton (HN) and nitrogen resonances with side chain Hβ proton signals; LEM, linear extrapolation model; *ec*HPr, histidine-containing protein from *Escherichia coli*; *bs*HPr, histidine-containing protein from *Bacillus subtilis*; sd, standard deviation; PTS, phosphoenolpyruvate:sugar phosphotransferase system.

S0006-2960(96)00349-2 CCC: $12.00

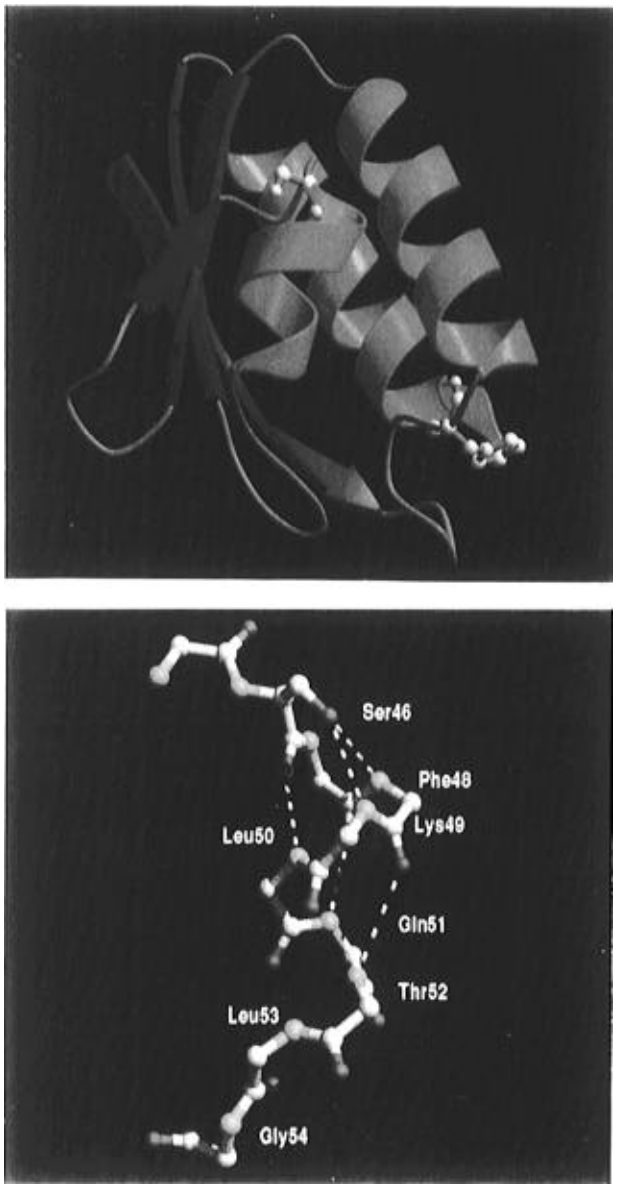

FIGURE 1: (a, top) Ribbon drawing of the folding topology of the *E. coli* HPr crystal structure (PDB code 1POH). The side chains of His15 and Ser46 have been depicted in a ball-and-stick representation. The image was prepared using MOLSCRIPT (Kraulis, 1991). (b, bottom) Ball-and stick representation of helix B from the *E. coli* HPr crystal structure for which Ser46 is the N-cap. Side chain−main chain hydrogen-bonding interactions between the Ser46 O^{γ} atom and the amides of Phe48 and Lys49 have been illustrated. Main chain H-bonding interactions have also been shown. This figure was prepared using the software package MidasPlus (Bash et al., 1983; Ferrin et al., 1988; Huang et al., 1991) from the Computer Graphics Laboratory, University of California, San Francisco.

X-ray structure while NMR studies have suggested that helix B is dynamically averaged in solution (Hammen et al., 1991; Wittekind et al., 1992). Backbone amide protons in helix B exchange rapidly compared to helices A and C and are not significantly protected from exchange in either *E. coli* or *Bacillus subtilis* HPrs. The solution structure of *B. subtilis* HPr (*bs*HPr) has recently been refined using NOE constraints from 3D ^{15}N- and ^{13}C-edited spectra, and the resulting structure confirms the presence of a short helix between residues Gly49 and Leu53 (B. Jones and R. Klevit, unpublished results).

Here we report the effect of substituting the N-cap residue of helix B, Ser46, on the local and global stability of *E. coli* HPr (*ec*HPr). We have chosen to focus on Ser46 for two reasons. First, as mentioned above, helix B is the shortest helix in the protein and shows signs of dynamic averaging in solution. Therefore, we reasoned that changes in the effectiveness of N-capping for this helix would more likely lead to significant effects on local stability. Second, helix B is implicated in important functional aspects of HPr, comprising part of the protein−protein interaction site between HPr and its phosphoacceptor protein, enzyme IIA (van Nuland, 1993; Chen et al., 1993) and between HPr and its phosphodonor, enzyme I (van Nuland et al., 1995). In addition to the phosphorylation on His15 that occurs as part of the phosphotransfer activity of the PTS, HPrs from Gram-positive organisms such as *B. subtilis* can also be phosphorylated on Ser46 by an ATP-dependent protein kinase, making them poor substrates of enzyme I of the PTS (Deutscher & Saier, 1983; Reizer et al., 1989). Phosphorylation of Ser46 on HPr from *B. subtilis* leads to a significant stabilization of helix B and to a global stabilization of the protein, in the absence of any detectable conformational change (Pullen et al., 1995). Substitution of Ser46 with aspartic acid in *bs*HPr mimics the functional aspects of phosphorylation and provides a similar stabilization to the protein. Although HPr from *E. coli* contains a serine at position 46, it cannot be phosphorylated at this position. However, substitution of Ser46 with aspartic acid also makes this HPr a poor substrate of enzyme I in its PTS (Napper et al., 1996). Therefore, to understand the mechanism by which mutation of Ser46 inhibits phosphocarrier properties of *ec*HPr, we have replaced Ser46 with Asp, Asn, and Ala in S46D, S46N, and S46A HPrs, respectively. The effect of mutating Ser46 on local and global stability of *ec*HPr has been determined using NMR spectroscopy and chemical and thermal denaturation studies, monitored by circular dichroism.

MATERIALS AND METHODS

Protein Expression and Purification. The expression and purification of wild-type and mutant HPrs in *E. coli*, both unlabeled and uniformly labeled with ^{15}N, have been previously described (Sharma et al., 1991).

NMR Sample Preparation. NMR samples were prepared as previously described (Hammen et al., 1991). The pH values reported for hydrogen exchange are corrected for isotope effects. Final protein concentration ranged from 1 to 4 mM, depending on the experiment.

NMR Spectroscopy. NMR spectra of wt and mutant HPrs were acquired on Bruker AM 500 and DMX 500 spectrometers operating at 500.13 MHz for ^{1}H and 50.68 MHz for ^{15}N. The sample temperature was maintained at 27 °C unless stated otherwise. For most experiments, quadrature detection in the t_1 dimension was implemented through the time-proportional phase increment method (Marion & Wüthrich, 1983). The proton spectral width was 10 000 Hz for homonuclear experiments and 7002 Hz for heteronuclear experiments. The ^{1}H and ^{15}N transmitters were set to 4.6 and 114.2 ppm, respectively. 2D NMR spectra were processed using FELIX 2.3 (Biosym Technologies, Inc.) software. Final real 2D matrices were typically 1024 points in t_1 and 2048 points in t_2, and the FIDs were weighted by

a squared sine-bell window shifted by $\pi/3$ prior to Fourier transform. The data were zero-filled to 1024 in t_1 before apodization, and all spectra were baseline corrected using a second- or third-order polynomial.

For S46D HPr, 2D homonuclear NOESY ($\tau_m = 200$ ms) and TOCSY (70 ms) spectra were acquired in H_2O and ^2H_2O using standard pulse sequences. Solvent suppression was achieved by presaturation during the 1.5 s relaxation delay. In addition, 2D $^{15}N-^1H$ HMQC-TOCSY and $^{15}N-^1H$ HMQC-NOESY spectra were collected for all three mutants, with NOESY and TOCSY mixing periods of 100 and 75 ms, respectively. Pulsed field gradients were used for water suppression. Given the limited chemical shift perturbations observed in spectra collected for the mutant proteins, assignments could be made in a straightforward manner by comparison with spectra of wt HPr.

$^3J_{NH\alpha}$ coupling constants were determined from *J*-modulated $^{15}N-^1H$ COSY experiments (Billeter et al., 1992). Using the modified pulse sequence of Neri et al., (1990), 12 *J*-modulated $^{15}N-^1H$ COSY spectra were recorded with variable delay (τ_2) values of 26, 52, 60, 68, 76, 84, 92, 100, 108, 116, 132, and 140 ms. The delay τ_1 used for the evolution of $^1J_{NH}$ couplings was tuned to 4.6 ms [$<(1/2)^1J_{NH}$]. The data size was 128 points in t_1 and 1024 points in t_2. A total of 64 transients were required for phase cycling. Presaturation by selective irradiation at the water frequency before each scan was used for solvent suppression. Values of $^3J_{NH\alpha}$ couplings were determined (Billeter et al., 1992) using a nonlinear least-squares program (NonLin, version 6.0) implemented for a Silicon Graphics computer. The values obtained for wt HPr were consistent with those determined earlier from $^{15}N-^1H$ HMQC-*J* spectra (Hammen et al., 1991).

Vicinal $^3J_{\alpha\beta}$ coupling constants were obtained from a PE COSY experiment (Mueller, 1987) collected using the States method (States et al., 1982) for quadrature detection. The spectra were acquired with 1024 t_1 increments ($t_{1,max} = 156$ ms) and zero-filled to yield a digital resolution of 1.2 Hz per point. Cross-peak patterns from 2D HNHB experiments (Archer et al., 1991) were analyzed to confirm specific χ_1 rotamers. HNHB spectra were acquired with the States−TPPI method (Marion & Wüthrich, 1989) for quadrature detection.

For quantitative comparison of NOE intensities between wt and S46D HPrs, ^{15}N-edited 3D NOESY-HSQC spectra were collected with 512 × 200 × 48 complex points and a mixing time of 120 ms. By comparing NOESY and ROESY spectra, we have determined that spin diffusion begins to occur at 150 ms for HPr (Hammen and Klevit, unpublished results). NOESY spectra were acquired with WATERGATE (using a 3-9-19 pulse sequence) for water suppression to minimize the attentuation of cross-peaks due to cross-saturation from H_2O to amide protons.

Hydrogen exchange rates of slowly exchanging amide protons were measured by $^1H-^2H$ exchange. The rate of disappearance of ^1H resonances due to exchange was monitored by a series of short (10.5 min) $^{15}N-^1H$ HSQC correlation spectra (Norwood et al., 1990) using pulsed field gradients to suppress the residual solvent signal. The first spectrum was initiated 5 min after the addition of ^2H_2O, and spectra were collected up to 6.5 h after addition of ^2H_2O. Pseudo-first-order rate constants were determined by fitting measured peak volumes to a single exponential rate equation using the program SigmaPlot for the MacIntosh. The slowest exchange rate accurately measured was 1.5×10^{-4} s^{-1}.

The measurement of exchange rates of rapidly exchanging amide protons ($k_{ex} \geq 1$ s^{-1}) was carried out by the method of Spera et al. (1991). Two identical $^{15}N-^1H$ HMQC spectra were recorded; one was recorded with presaturation of the water signal between scans whereas the other employed a 1-1 echo for solvent suppression. Pairs of spectra were recorded at 27 °C at four different pH values: 6.5, 7.0, 7.7, and 8.5. Hydrogen exchange rates were calculated at pH 7.4, as outlined in Spera et al. (1991).

Intrinsic hydrogen exchange rates (k_{int}) were calculated at the specific experimental pH and temperature conditions by the method of Bai et al. (1993). These values were used for calculation of protection factors (*P*) for individual amides which is defined as the ratio k_{int}/k_{obs}. The difference in free energy, $\Delta\Delta G_{HX}$, was determined for the mutant proteins by using protection factors determined for the helical residues Lys49, Leu50, and Gln51.

For 1D NMR studies, ^{15}N resonances were directly observed using a 5 mm broad-band probe. The spectral width was 20 000 Hz, and the carrier was placed at 200 ppm. A total of 2000−5000 transients were acquired. The chemical shift of ^{15}N was referenced to liquid ammonia. For wt and S46D HPrs, pH titration of histidine C^ϵ protons was carried out from pH* 4.66−9.66 in increments of 0.2 pH* units to compare the pK_as of His15 and His76. The pK_a value was determined by fitting the chemical shift of histidine $C^\epsilon H$ resonances as a function of pH* to the Henderson−Hasselbalch equation: $\delta_i = \delta_{His} + (\delta_{His^+} - \delta_{His})\{10^{n(pK-pH)}/[1+ 10^{n(pK-pH)}]\}$, where n is the Hill coefficient, δ_i the weighted average of the imidazole chemical shift δ_{His} and the imidazolium chemical shift δ_{His^+} (Markley, 1975).

Protein Denaturation Studies. For both thermal- and urea-denaturation experiments, the unfolding transition was monitored by circular dichoism (CD) at 222 nm using an Aviv 62DS spectropolarimeter equipped with a temperature control and stirring unit. Thermal unfolding curves were performed with heating rates from 30 to 45 °C per hour in cuvettes with path lengths of 1 or 10 mm.

For the urea-denaturation curves, the urea solutions were prepared fresh daily in buffered solutions containing 10 mM potassium phosphate at pH 7.0. The concentration of the urea stock solution was determined by refractive index measurements (Pace, 1986). Since the folding equilibrium was reached rapidly for the wild-type protein and the mutants studied here, the urea-denaturation curves were performed using the method of serial additions of urea to a protein sample with a correction made for the increase in volume as described by Scholtz (1995).

A complete description of the data analysis performed on the urea and thermal denaturation experiments has been described (Scholtz, 1995). The changes in ΔG for each mutant protein compared to the wild-type protein ($\Delta\Delta G$) were calculated by two methods. The first, using urea denaturation data, calculated the change in ΔG by $\Delta\Delta G = \langle m \rangle \cdot \Delta C_{mid}$, where $\langle m \rangle = 1090$ cal mol^{-1} M^{-1}, the average *m*-value from all the urea-denaturation curves of the wild-type and variants of the *ec*HPr protein, and ΔC_{mid} is the difference in midpoint of the transition relative to wild-type protein. The changes in ΔG from the analysis of the thermal unfolding data were determined by the relationship described by Becktel and Schellman (1987): $\Delta\Delta G = \Delta T_m \cdot \Delta H_m(wt)/$

T_m(wt), with T expressed in kelvin. Both methods assume a two-state unfolding reaction. In addition, the analysis of the urea-denaturation curves assumes a linear relationship between free energy of folding and the molar concentration of urea (linear extrapolation method), while the analysis of the thermal-unfolding curves assumes a constant ΔC_p for the proteins.

RESULTS

Effect of Mutagenesis on Overall Structure. Since Ser46 is a solvent-exposed N-cap, our hypothesis was that single amino acid substitutions at this position would not cause large conformational changes in the protein. Consistent with this hypothesis, analysis of NOEs, coupling constants, and exchange rates from 2D and 3D NMR experiments gave strong indications that there was no change in the overall topology of *ec*HPr when Ser46 was mutated to Asp, Asn, or Ala (Table 1). The pK_as of the two histidines, His15 and His76, were determined in S46D HPr and found to be indistinguishable from wt [pK_a of His15, 5.6 (wt), 5.5 (S46D); pK_a of His76, 6.2 (wt), 6.1 (S46D); sd ±0.1]. Direct detection of ^{15}N side chain resonances of the active site residues His15, Arg17, and Pro18 also showed no change in the chemical shift of these resonances (data not shown). These observations indicate that (i) substitutions at Ser46 do not cause global structural changes in HPr and (ii) the loss of phosphotransfer activity in *E. coli* S46D (Napper et al., 1996) cannot be attributed to either the inability of HPr to attain the proper fold or a change in the conformation or electronic environment around the active site His15.

Effect of Mutagenesis on Local Conformation. We compared a variety of NMR parameters capable of detecting small structural differences that might exist in the mutant proteins: chemical shifts, $^3J_{NH\alpha}$ and $^3J_{\alpha\beta}$ coupling constants, and NOE intensities. Complete backbone and side chain assignments were obtained for the three mutants. As illustrated in Figures 2 and 3, the chemical shift perturbations of backbone amide proton and ^{15}N resonances are small and localized to the site of mutation. Interestingly, side chain N$^{\epsilon}$ resonances of Gln51 are also perturbed in S46D HPr (Figure 2). Chemical shifts of residues near the active site His15 are largely unaffected. A comparison of perturbations observed for S46D and S46N reveals that the magnitude and direction of chemical shift perturbations are similar in both proteins. This suggests that the chemical shift perturbations are not simply due to the presence of a negative charge and that similar conformational or dynamic changes may occur in S46D and S46N. The amide resonances of Lys49 and Leu50, which represent amides $i + 3$ and $i + 4$ in helix B, experience downfield shifts in S46D and S46N while the same resonances are shifted upfield in S46A. The large upfield shift of Lys49 by 0.8 ppm (^{1}H) in S46A is noteworthy, since downfield shifts of amide proton resonances are often associated with hydrogen bond formation. Other than Lys49 and Leu50, none of the residues removed from the site of mutation are significantly perturbed in S46A HPr.

The $^3J_{NH\alpha}$ coupling constant is empirically correlated to the ϕ backbone dihedral angle through the Karplus relationship (Karplus, 1959; Pardi et al., 1984). $^3J_{NH\alpha}$ <6 Hz correlate with ϕ angles of −40° to −80° and are therefore indicative of α-helical structure; $^3J_{NH\alpha}$ >8 Hz associate with ϕ angles of −100° to −160° and are indicative of β-sheets. As shown in Table 1, the measured $^3J_{NH\alpha}$ coupling constants for wt HPr correlate well with regular secondary structure observed in the crystal structure. A residue-by-residue comparison of the measured coupling constants in wt and S46D HPrs gave an average standard deviation of ±0.2 Hz. Only one residue showed a difference greater than 2 sd: Phe48 increases 1.4 Hz from $^3J_{NH\alpha} = 3.7 \pm 0.1$ Hz in wt HPr to 4.9 ± 0.1 Hz in S46D. Thus the coupling constants detect only a minor change in backbone conformation within helix B in the mutant protein.

The coupling constants determined for wt HPr highlight the irregular nature of helix B in the native protein. Coupling constants between 6 and 8 Hz can either be indicative of ϕ angles between −80° and −100° and/or conformational averaging due to rotation about the N−C$^{\alpha}$ bond. Lys49, Thr52, and Leu53 in wt HPr have coupling constants of 6.5, 7.5, and 6.7 Hz, respectively (Table 1), and these couplings have previously been interpreted as indicating conformational averaging in this region (Hammen et al., 1991). However, in the refined *ec*HPr crystal structure (Jia et al., 1993), Thr52 and Leu53 adopt dihedral angles that are outside of the α-helical range: (ϕ, ψ) of (−89°, −8°) and (−92°, +157°), respectively. If these angles are adopted in solution, the Karplus equation would predict coupling constants of 8.6 and 8.1 Hz. Thus, the measured nonhelical coupling constants cannot be unambiguously attributed to conformational averaging, since they are also consistent with a somewhat distorted conformation as observed in the crystal (Jia et al., 1993). Nevertheless, our solution data indicate that regular α-helical structure ends at Thr52 in wt and mutant HPrs. This is also consistent with the length of helix B reported in the *ec*HPr solution structure (van Nuland et al., 1994) where the authors state that helix B extends from residues 47 to 52.

The presence of a helix in solution is also characterized by a string of sequential d_{NN} NOEs as well as medium range (i, $i + 3$) NOEs. In wt HPr, residues Ala44−Thr52 are connected by strong d_{NN}s, consistent with the presence of helical structure in this region. The d_{NN} between Thr52 and Leu53 lies too close to the diagonal to be identified with certainty whereas a weak d_{NN} is present between Leu53 and Gly54. In addition, four medium-range NOEs can be unambiguously identified between Lys49α−Thr52NH, Lys49α−Leu53NH, Leu50α−Leu53NH, and Leu50α−Thr52NH protons. To compare NOE differences between S46D and wt, the ratio of NOE intensities S46D/wt was determined (see Materials and Methods) for 134 short- and medium-range cross-peaks for residues Ala42−Thr59 and the active site. The ratios were close to 1.0 (standard deviation, 0.8) for all NOEs analyzed.[2] We therefore concluded that no significant NOE differences were observed between wt and S46D HPrs.

Side chain rotamer conformations, as characterized by the dihedral angle χ_1, were analyzed by PE COSY and HNHB

[2] A quantitative comparison of peak intensities from apparantly "identical" NOESY spectra yielded average relative errors in intensity as high as 64% which correspond to only 10% relative error in distance, due to the r^{-6} relationship to NOESY peak intensity (Hoffman et al., 1993). Furthermore, for the data sets analyzed in the present work, the ratio between the highest intensity peak and the lowest intensity peak (which corresponds to a distance of 3.8 Å in the crystal structure) is 35.0.

Table 1: $^3J_{NH\alpha}$ and Logarithms of the Amide Proton Protection Factors for *E. coli* wt, S46D, S46N, and S46A HPrs[a]

	$^3J_{NH\alpha}$[b]		log *P*				
residue	wt	S46D	wt	S46D	S46N	S46A[c]	secondary structure[d]
Phe2	8.9	8.9	§[b]	§	§	§	*β*-A
Gln3	8.4	8.5	1.8−4.0	1.8−4.0	1.8−4.0		*β*-A
Gln4	7.6	7.6	>5.3	>5.3	>5.3		*β*-A
Glu5	8.7	8.7	2.6	2.7	2.7		*β*-A
Val6	8.1	8.1	>4.9	>4.9	>4.9		*β*-A
Thr7	8.7	9.1	2.9	3.2	2.7		*β*-A
Ile8	6.3	6.3	>4.8	>4.8	>4.8		*β*-A
Thr9	10.0	9.8	1.5	1.5	1.5	1.6	
Ala 10	3.2	3.2	4.1	4.1	4.1		
Pro11							
Asn12	9.0	8.7	1.5	1.5	1.5	1.7	
Gly13			1.9	1.9	1.9	1.9	
Leu14	9.0	8.8	2.5	2.4	2.5	2.5	
His15	*f*	*f*					
Thr16	<3.6	<3.6	1.5	1.6	1.5	1.4	
Arg17	4.0	4.9	2.5	2.4	1.9	2.0	α-A
Pro18							α-A
Ala19	4.1	3.8	1.5−3.8	1.5−3.8	1.5−3.8		α-A
Ala20	3.9	3.9	1.7−4.0	1.7−4.0	1.7−4.0		α-A
Gln21	5.5	5.5	1.7−4.0	1.7−4.0	1.7−4.0		α-A
Phe22	3.3	3.2	3.9	3.9	3.9		α-A
Val23	§	§	§	§	§	§	α-A
Lys24	4.1	4.3	4.7	4.7	4.7		α-A
Glu25	5.7	5.6	4.7	4.8	4.8		α-A
Ala26	3.1	3.1	>5.5	>5.5	>5.5		α-A
Lys27	3.8	3.8	5.4	5.5	5.4		α-A
Gly28			3.4	3.4	3.3		
Phe29	9.8	9.8	5.2	5.0	5.0		
Thr30	7.7	7.6					
Ser31	2.7	1.9	4.2	4.2	4.3		
Glu32	8.6	8.7	2.5	2.5	2.8		*β*-B
Ile33	9.4	9.6	§	1.6	1.5	1.5	*β*-B
Thr34	9.8	9.6	>5.2	>5.2	>5.2		*β*-B
Val35	9.7	10.2	>4.9	>4.9	>4.9		*β*-B
Thr36	9.8	10.6	>5.6	>5.6	>5.6		*β*-B
Ser37	7.6	7.7	4.6	4.5	4.7		
Asn38	*f*	*f*	¶	¶	¶	¶	
Gly39			¶	¶	¶	¶	
Lys40	9.7	9.8	>5.6	>5.6	>5.6		*β*-C
Ser41	9.6	8.8	1.4	1.3	1.3	1.4	*β*-C
Ala42	8.2	8.0	4.1	4.1	4.1		*β*-C
Ser43	3.8	4.0	0.9	1.4	0.9	0.9	*β*-C
Ala44	4.8	4.5	4.4	5.6	4.6		*β*-C
Lys45	8.9	8.9	4.2	4.2	4.2		
46	9.6	10.0	3.7	3.7	4.0		
Leu47	*f*	2.8	¶	**1.8−4.0**	1.5	¶	α-B
Phe48	**3.7**	**4.9**	**0.8**	**2.1**	**1.6**	**0.6**	α-B
Lys49	6.5	6.3	**1.3**	**2.2−4.5**	**2.2−4.5**	**1.4**	α-B
Leu50	2.9	2.9	**2.4−3.7**	**4.0**	**3.5**	**1.7**	α-B
Gln51	§	4.8	**1.7−3.0**	**3.6**	**3.1**	**2.2**	α-B
Thr52	7.5	7.5	1.9	1.9	1.9	1.5	α-B
Leu53	6.7	6.4	2.9	2.8	3.0		
Gly54			0.9	0.6	1.0	1.1	
Leu55	7.9	7.5	1.4	1.4	1.5	1.6	
Thr56	§	7.9	2.3	2.1	2.3	2.2	
Gln57	<3.6	<3.6	1.6	1.8	1.7	1.8	
Gly58			3.9	3.8	4.0		*β*-D
Thr59	§	§	>5.2	>5.2	>5.2		*β*-D
Val60	8.8	8.7	2.7	2.9	3.0		*β*-D
Val61	10.0	9.5	>4.9	>4.9	>4.9		*β*-D
Thr62	9.9	9.8	>5.1	>5.1	>5.1		*β*-D
Ile63	10.5	9.0	§	§	§	§	*β*-D
Ser64	9.8	9.7	>5.7	>5.7	>5.7		*β*-D
Ala65	8.8	8.8	>5.2	>5.2	>5.2		*β*-D
Glu66	§	§	§	§	§	§	*β*-D
Gly67			4.2	4.1	4.3		
Glu68	*f*	2.7	¶	¶	¶	¶	
Asp69	10.1	10.4	1.5	1.5	1.5	1.8	α-C
Glu70	3.4	3.4	4.4	4.4	4.5		α-C
Gln71	5.3	5.1	4.7	4.8	4.7		α-C
Lys72	4.3	4.3	3.5	3.3	3.3		α-C
Ala73	2.9	2.9	§	§	§	§	α-C
Val74	4.6	4.6	>4.5	>4.5	>4.5		α-C

Table 1 (Continued)

	$^3J_{NH\alpha}$[b]		log *P*				
residue	wt	S46D	wt	S46D	S46N	S46A[c]	secondary structure[d]
Glu75	3.7	3.3	>5.7	>5.7	>5.7		α-C
His76	4.2	4.2	>6.0	>6.0	>6.0		α-C
Leu77	5.2	5.4	2.7	3.0	2.9		α-C
Val78	4.4	4.4	>4.8	>4.8	>4.8		α-C
Lys79	4.6	4.4	3.8	4.2	4.0		α-C
Leu80	4.1	3.7	§	§	§	§	α-C
Met81	3.8	3.8	>5.4	>5.4	>5.4		α-C
Ala82	5.2	5.4	4.2	4.3	4.3		α-C
Glu83	8.8	8.8	2.7	2.8	2.6		α-C
Leu84	4.4	4.2	2.6	2.6	2.6		α-C
Glu85	8.4	8.4	4.1	4.4	4.3		

[a] Residues that show a significant difference among the proteins studied are shown in bold type. Symbols used are as follows: §, value is not determined due to spectral overlap; ¶, attenuation (M_o/M_{ps}) measured in 1:1 vs presaturation experiments is too large for accurate measurement; *f*, coupling constant is not measured due to exchange broadening. [b] The average standard error determined from the fits was 0.1−0.2 Hz, and the overall sd for all couplings determined was 0.2 Hz. [c] For S46A, exchange rates for only fast exchanging amides were determined due to sample limitations. [d] Secondary structure designation is based on Jia et al. (1993).

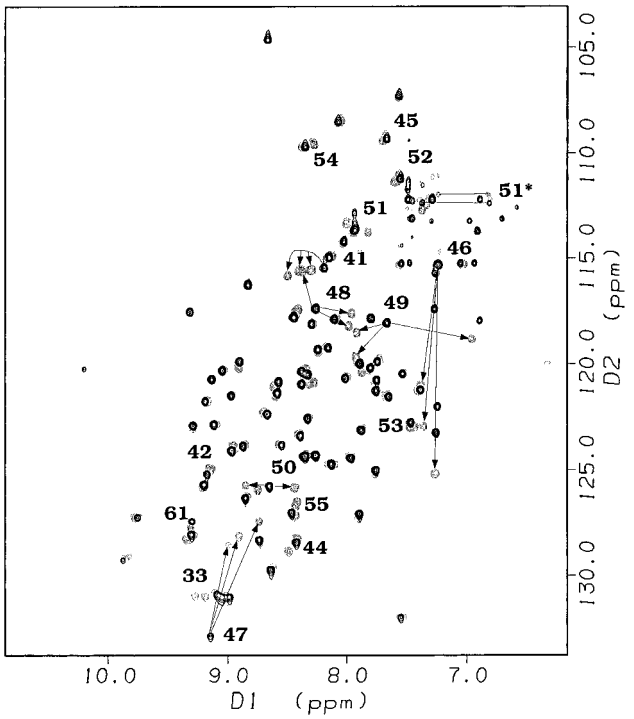

FIGURE 2: ^{1}H, ^{15}N HSQC spectra of wt (black) and mutants (gray) are overlaid to show the extent of backbone chemical shift perturbations. All spectra were collected at pH 6.5 and 30 °C.

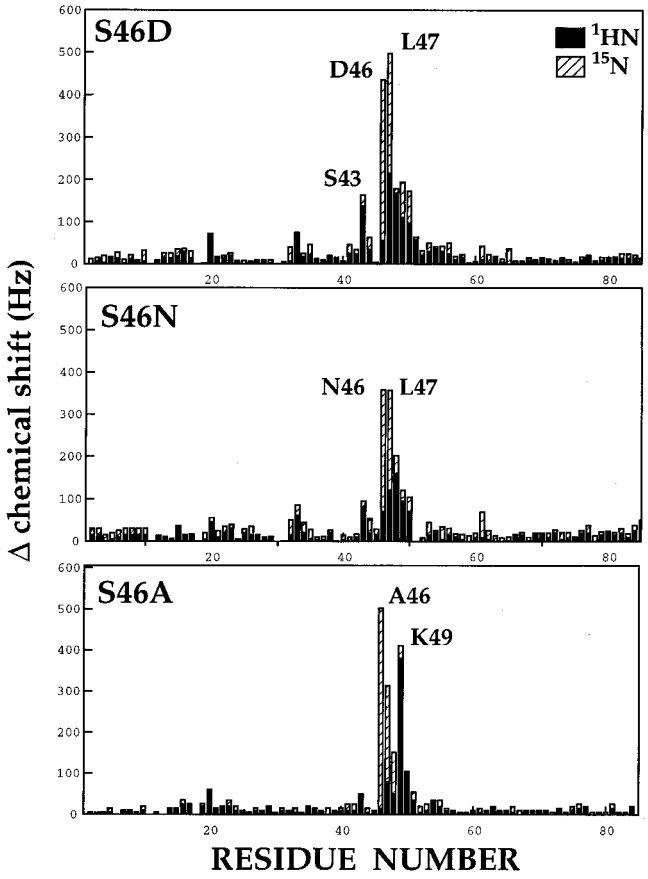

FIGURE 3: Comparison of the total (^{1}HN + ^{15}N) magnitude of chemical shift perturbations (in hertz) between the three mutants. Values shown represent the absolute difference $|\delta_{wt} - \delta_{S46X}|$, where black bars indicate the perturbation in amide proton and hatched bars the perturbation observed in ^{15}N.

spectra, as summarized in Table 2. Where measurable in both forms, the side chain rotamer conformations for residues with prochiral C$^\beta$s do not change detectably between wt and the S46X mutants. The prochiral C$^\beta$ resonances of helix B residues Ser46, Lys49, and Gln51 are degenerate in wt HPr (Table 2), and therefore their χ_1 rotamers cannot be determined. Such degeneracy may indicate conformational averaging of these side chains in the native protein. Consistent with this, Ser46 C$^\beta$s (3.85 ppm) resonate close to the random coil chemical shift (3.82 ppm) (Wüthrich, 1986). In contrast, the C$^\beta$ resonances of residue 46 in S46D and S46N are well resolved, with differences in chemical shift between the two β-protons of 0.9 ppm in S46D and 0.6 ppm in S46N. These differences are large when compared to random coil values for Asp and Asn residues (Δ^β_{shift} Asp = 0.09 ppm; Δ^β_{shift} Asn = 0.08 ppm) and suggest that residue 46 is conformationally constrained in the mutants. On the basis of the observed $^3J_{\alpha\beta}$ coupling constants, NOE patterns, and HNHB spectra, Asp46 and Asn46 are expected to exist as *trans* rotamers (+180°) in solution. In contrast to Ser46, the β-protons of Phe48 are well resolved in wt HPr and become almost degenerate in both S46D and S46N mutants. In the S46D *ec*HPr crystal structure (Napper et al., 1996), the authors report a change in conformation for the Phe48 side chain. These results, in addition to the increased $^3J_{NH\alpha}$ coupling constant observed for Phe48 in S46D, suggest that small, subtle changes in conformation occur around residue 46 upon mutation.

Table 2: Comparison of the Angle χ_1 (deg) for Residues in Helix B of wt and Mutant HPrs

residue	wt	S46D	S46N
S/D/N46	degenerate	180	180
L47	*a*	*a*	*a*
F48	averaged	averaged	averaged
K49	degenerate	degenerate	degenerate
L50	−60	−60	−60
Q51	averaged	averaged	averaged
L53	−60	−60	−60

[a] The β-methylene protons of L47 are absent from all three spectra due to rapid exchange of the L47 NH. Residue 52 has not been included since it is a Thr. No difference in χ_1 was found for any other residue in wt and S46X HPrs.

Effect of Mutagenesis on Amide Exchange. The chemical exchange of backbone amide protons with solvent gives information concerning hydrogen bonding and solvent accessibility and is a useful tool for the study of backbone dynamics in proteins. There are roughly three regimes of amide exchange that can be studied by NMR. Slowly exchanging amide protons are those that persist long enough to be detected after the addition of ^2H_2O in a $^1H-^2H$ exchange experiment. Under the conditions employed in our studies, amide protons that exchange slower than 0.05 s^{-1} can be measured by this approach. Fast exchanging amide protons are those that exchange at a rate greater than 1 s^{-1}, and these were analyzed by a method that utilizes transfer of saturation from water to amide protons (Spera et al., 1991). The third category consists of amide protons that exchange in the intermediate regime of 0.05−1 s^{-1}, and exact rate constants for these residues cannot be determined by the methods employed herein.

Under conditions that favor the folded state, amide protons of most globular proteins are expected to exchange by the EX_2 mechanism (Hvidt & Nielson, 1966; Wagner, 1983; Wand, 1986). This mechanism proposes that, during transient local unfolding, the rate of closure is faster than the rate of exchange in the open state and the experimentally determined hydrogen exchange rate is therefore pH dependent. The protons of helix B show a strong pH-dependent increase in exchange rate (data not shown), so we can presume that exchange occurs mostly by the EX_2 mechanism. Hence, in the absence of a conformational change, we attribute a significant decrease in hydrogen exchange rate due to mutagenesis to (i) an increase in the rate of closure or increase in the lifetime of the closed state or (ii) a steric or inductive effect of a neighboring side chain. Protection factors, defined as k_{int}/k_{obs} (see Materials and Methods), take steric and inductive influences of neighboring side chains on amide exchange into account (Bai et al., 1993), and these have been calculated for all amides in native and mutant HPr proteins, as summarized in Table 1. The protection factors for wt HPr show that whereas amides in β-strands and helices A and C are well protected from solvent, helix B residues Leu47−Thr52 have among the lowest protection factors in the protein. With the exception of residues near the site of mutation, most protection factors in the mutants are the same, within experimental error, as those in wt HPr. Residues Ala44, Leu47, Phe48, Lys49, Leu50, and Gln51 show significant changes in one or more of the Ser46 mutants, with protection factors increasing in S46D and S46N and decreasing in S46A. The largest increases are observed in helix B residues in S46D. The amides of Phe48 and Lys49, both potential H-bond donors to the N-capping side chain, are at least 20-fold more protected in wt HPr. Slightly smaller protections for these groups are observed in S46N. Surprisingly, substitution of the putative N-cap with alanine does not significantly decrease the protection of Phe48 and Lys49 relative to wt HPr. This suggests that, in the native protein, the putative hydrogen bond between the Ser46 O^γ and the NH of Lys49 does not afford much protection against exchange. The amide proton of Leu47 is not predicted to participate in a H-bond, yet it is also protected ∼20-fold in S46D and S46N. The large upfield shift experienced by the Leu47 resonance in the mutants is not consistent with the formation of a new H-bond and suggests that the protection of this amide may be due to a steric effect.

The highest protection factors and the largest effects on exchange are for the amides of Leu50 and Gln51. In wt HPr, Leu50 and Gln51 exchange too rapidly to be observed in the first HSQC spectrum after $^1H-^2H$ exchange, while these resonances persist for more than 1 h in S46D. The protection factor for Leu50 is increased at least 40-fold relative to wt HPr. Again, smaller increases are observed for the S46N mutant. In contrast, the protection factors for both residues are decreased when serine is replaced by alanine at the N-capping position. These two amides are predicted to participate in main chain−main chain H-bonds with the carbonyls of residue 46 and Leu47, and the effects observed in the mutants suggest a stabilization of the helical structure for S46D and S46N and a destabilization of helical structure in S46A.

Effect of Mutagenesis on Stability. The global conformational stability of each of the four proteins was determined in two different ways. Thermal unfolding curves were analyzed to afford a measure of the difference in conformational stability near the midpoints of the thermal transitions (58−69 °C), and urea-denaturation curves were used to determine the differences in stability at 30 °C. Each method gives nearly identical results, suggesting that the assumptions used in the analysis of the data and the models employed for the analysis are valid. Figure 4A shows the urea-denaturation curves for the four proteins. For all these proteins, and from repeated measurements of urea denaturation curves on the wild-type protein at various temperatures, we find an *m*-value of 1090 cal mol^{-1} M^{-1} satisfactorily fits all available data (Nicholson & Scholtz, 1996). The differences in global conformational free energy ($\Delta\Delta G°$) can, therefore, be determined from the relationship (see Materials and Methods):

$$\Delta\Delta G° = \langle m \rangle \cdot \Delta C_m \qquad (1)$$

where $\langle m \rangle$ represents the average *m*-value for *ec*HPr and ΔC_m is the difference in midpoints of the unfolding curves. This analysis shows that S46D and S46N are more stable than wt HPr by 1.5 and 0.5 kcal mol^{-1}, respectively, and S46A is less stable than wt HPr by 0.9 kcal mol^{-1}. Table 3 shows the results of this analysis for the four proteins.

Thermal unfolding curves were also performed on the four proteins (Figure 4B). These curves were analyzed using the method of Becktel and Schellman (1987) to afford a measure of differences in conformational stability at higher temperatures (see Materials and Methods). The results of this analysis are also shown in Table 3. There is excellent

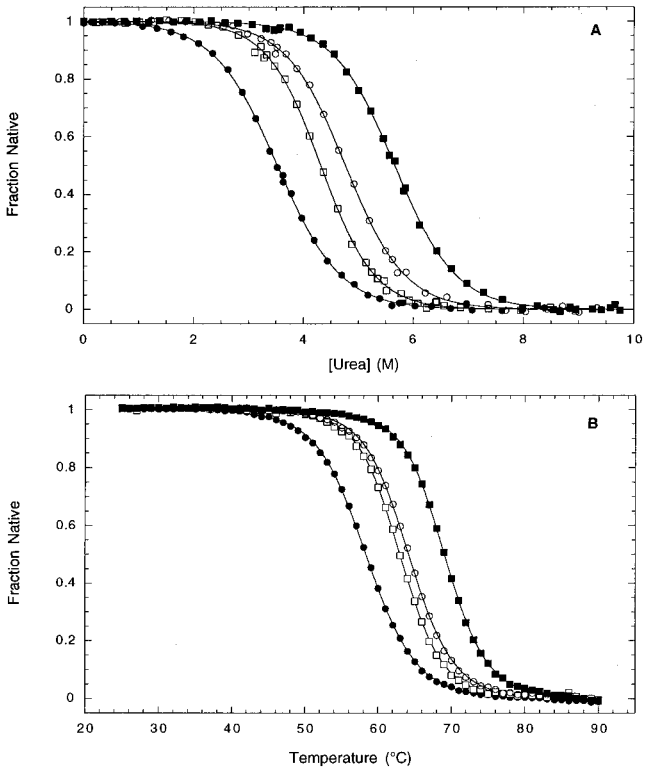

FIGURE 4: Urea (A) and thermal (B) denaturation curves for the HPr variants: wild type (□), S46D (■), S46N (○), and S46A (●). The transitions were monitored by circular dichroism. The lines through the data are derived from the simple models for the transitions (see text).

Table 3: Comparison of $\Delta\Delta G^{unf}$ from Thermal Unfolding and Urea Denaturation to $\Delta\Delta G_{HX}$ from Hydrogen Exchange (kcal/mol)

method	S46D	S46N	S46A
thermal unfolding	$+1.4 \pm 0.2$	$+0.3 \pm 0.2$	-1.1 ± 0.2
urea unfolding	$+1.5 \pm 0.2$	$+0.5 \pm 0.2$	-0.9 ± 0.2
NH exchange	$+(1.8-1.9)$	$+(0.8-1.5)$	$-(0.2-0.9)$

agreement between the differences in global conformational stability ($\Delta\Delta G°$) determined from the two methods.

DISCUSSION

Structural and Dynamic Consequences of N-Cap Substitutions. We have undertaken a detailed characterization of a putative N-cap residue in *ec*HPr. A comparison of NMR parameters shows that substitution of Ser46 is not accompanied by major structural changes and that observed differences are localized to helix B. Upon substitution of Ser46 by Asp or Asn, residues Leu47−Gln51 are protected from exchange by 10−40-fold. Since amide exchange appears to occur predominantly by the EX_2 mechanism, we rationalize that the increased protection from exchange is due to an increase in the lifetime of the helical conformation and hence local stabilization of helix B. Thus, the stability of helix B is directly influenced by mutations at the N-cap.

Protection factors can be used to calculate local changes in free energy for a protein: the difference in ΔG between wt and mutant HPrs is calculated as $\Delta\Delta G_{HX} = -RT \ln(P_{wt}/P_{mutant})$ (Bai et al., 1993; Loh et al., 1994). Under the experimental conditions used, a range of $\Delta\Delta G_{HX}$ values was calculated using the upper and lower limits of protection determined for several amides in helix B for S46D, S46N, and S46A HPrs, respectively (see Materials and Methods). The exchange experiments were performed under conditions similar to the urea and thermal denaturation, allowing comparison of $\Delta\Delta G_{HX}$ to the $\Delta\Delta G^{unf}$ measured from global unfolding (Table 3). Remarkably, these values lie within experimental error to those obtained from solvent or thermal denaturation, suggesting that the observed increase in global stability is related to the increase in local stability observed around residue 46. This result is an intriguing one since it is generally accepted that only the exchange of "core", highly protected hydrogens is strongly correlated with thermal stability (Roder, 1989; Wagner & Wüthrich, 1979). The equal increase in $\Delta\Delta G_{HX}$ and $\Delta\Delta G^{unf}$ due to mutagenesis at the N-cap suggests that local changes in free energy measured by hydrogen exchange experiments are correlated with the overall free energy change as measured in conformational stability studies. These results are also consistent with a hiearchial model for protein folding.

The influence of N-capping residues on helix B stability in *E. coli* HPr is in the order Asp > Asn > Ser > Ala. The NMR parameters of S46D and S46N suggest a mechanism by which these residues are helix stabilizing. In solution, both Asp46 and Asn46 side chains exist in a single staggered conformation (+180°), consistent with that observed in the crystal structures of S46D HPr from both *E. coli* and *B. subtilis*, in which a carboxylate oxygen of Asp46 is in H-bonding geometry with the amides of residue 49 and/or residue 48 (Liao & Herzberg, 1994; Napper et al., 1996). The increased protection factors and downfield shift of the Lys49 amide proton afforded by the substitution of either aspartate or asparagine suggest that an N-capping side chain to main chain H-bonding pattern exists in solution. The additional stabilization afforded by aspartate relative to asparagine either may be due to stronger H-bonding via a negatively charged oxygen versus the neutral oxygen of asparagine or could be due to a favorable interaction between the negatively charged side chain and the helix macrodipole. These effects are difficult to dissect, and both are likely to play a role.

Comparison of HPr Results with N-Capping Results from Other Studies. The first observation that certain amino acids are preferred at helix N- and C- termini was made by Richardson and Richardson (1988), who noted that Asn, Asp, and Ser are preferred at helix N-cap positions, whereas Gly is generally preferred at the helix C-cap. Since then, numerous studies have investigated the influence of charged and N-capping side chains in helix stability. Recently, Doig and Baldwin (1995) measured N-cap propensities for all 20 amino acids in alanine-based peptide models. Their results showed clearly that, in the absence of other side chain influences, Asp, Asn, and Ser afford the most stabilization at the N-cap position. The question arises: How well do results from peptide models correlate with the properties in intact proteins? There are two examples of proteins where the effect of N-cap substitutions on protein structure and stability has been investigated. Serrano and Fersht (1989) substituted the N-cap residues Thr6 and Thr26 with six other amino acids in barnase and observed that, in both helices, Asn was energetically less favorable relative to Thr or Ser. In T4 lysozyme, substitution of N-caps Ser38 and Asn144 by aspartic acid results in stabilization of the protein (Nicholson et al., 1988, 1991). Crystallographic studies of the two lysozyme mutants indicate that the hydrogen bond geometry at the N-cap is not optimal. Therefore, the increase

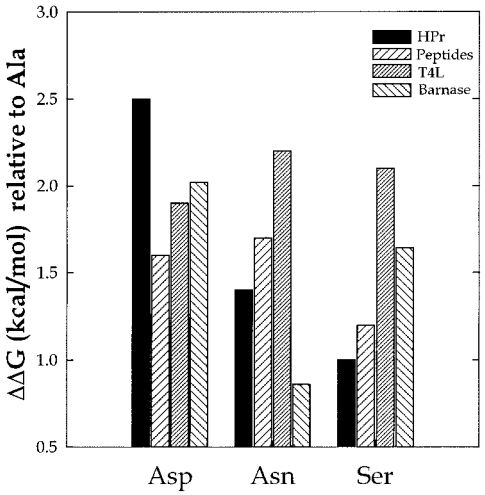

FIGURE 5: Comparison of relative unfolding free energies $\Delta\Delta G$ between *ec*HPr, T4 lysozyme (Bell et al., 1992), barnase (Serrano et al., 1992), and the peptides of Doig and Baldwin (1995).

in helix stability in these mutants was attributed to a favorable interaction of the negative charge with the helix macrodipole.

Normalized $\Delta\Delta G$ values relative to Ala are presented for Asp, Asn, and Ser N-caps in T4 lysozyme, barnase, peptide models, and HPr in Figure 5. Our results for HPr are in general agreement with those observed for T4 lysozyme (Nicholson et al., 1988); i.e., Asp and Asn are better N-capping residues than Ser. In *ec*HPr, both Asp46 and Asn46 appear to be good hydrogen bond acceptors in HPr. Our results for Ala to Ser and Ala to Asn mutations are also in good agreement with the substitutions in alanine-based peptide models (Doig & Baldwin, 1995; Doig et al., 1994). The major difference between the HPr protein data and the data from Doig and Baldwin is for Asp at the N-cap position. The greater stabilization afforded by Asp46 in *ec*HPr may be due in part to the proximity of the positively charged side chain of Lys49. The solution NMR spectrum does not, however, offer any positive evidence in support of a salt bridge interaction between the side chains of Asp46 and Lys49. The side chain proton resonances of Lys49 are not significantly perturbed in S46D HPr relative to wt HPr. In particular, the prochiral C^{β} protons are degenerate, which is more indicative of conformational averaging than of a single, fixed conformation expected for a stable side chain−side chain interaction. Furthur mutations will be required to determine the potential role of Lys49 in the stabilization of S46D. However, the agreement between the results in the peptide and protein system indicates that each are reporting the same event, namely, the stabilization of helical structure by favorable helix−dipole interactions and/or better hydrogen bonding as manifested in the N-cap propensities.

Comparison of E. coli S46D HPr with B. subtilis P-Ser46 HPr. HPr from *B. subtilis* and *E. coli* share ∼33% sequence identity, and their overall structures are very similar. In spite of their striking overall structural and sequence similarity, the ATP-dependent protein kinase that phosphorylates Ser46 in the *B. subtilis* protein will not phosphorylate the analogous residue in *ec*HPr. However, similar to the effect reported in *bs*HPr, substitution of Ser46 by aspartic acid makes the protein a poor substrate for His15 phosphorylation by enzyme I. Since the $C^{\alpha}-C^{\alpha}$ distance between His15 and Ser46 is ∼20 Å, it is of interest to know how such an inhibitory effect is mediated.

Recently, Pullen et al. (1995) described the effect of Ser46 phosphorylation on the structure and stability of *B. subtilis* HPr. Similar to the observations reported here for *E. coli* S46D HPr, an increase in both helix B stability and global stability was observed, in the absence of conformational change. This implies that although there are sequence differences between the two proteins, were *E. coli* HPr capable of being phosphorylated at Ser46, the structural and dynamic consequences would be similar to that observed in P-Ser46 HPr.

An intriguing difference in the two proteins is that the Asp in *ec*S46D is twice as stabilizing ($\Delta\Delta G$ = 1.5 kcal mol^{-1}) as either the Asp or the doubly negatively charged phosphoserine in *bs*HPr. In this context, we note that residue 49 is a lysine in *ec*HPr and a glycine in *bs*HPr. In addition, position 46 in *ec*HPr is surrounded by a number of positively charged residues, e.g., Lys45, Lys27, and Lys49, that are not present in *bs*HPr. Therefore, the presence of a negative charge may have a more favorable electrostatic component in *ec*HPr.

Comparison of E. coli S46D NMR and X-ray Structures. In general, there is good agreement between NMR data reported herein and the crystal structure of *E. coli* S46D HPr (Napper et al., 1996). Both X-ray and NMR studies show that mutation at Ser46 does not greatly affect the overall structure of HPr. In the accompanying paper the authors report a decrease in main chain H-bond length for residues comprising helix B which is consistent with the NMR results indicating a stabilization of helix B. There is, however, one significant difference between the two studies: the length of helix B increases to include Leu53 and Gly54 in the crystal structure whereas the NMR results show that increased protection from exchange is restricted to residues 46−51 in S46D HPr. Thus, the presence of a "better" N-cap in *ec*HPr does not appear to recruit additional residues into the helix in solution. The NMR data suggest that these residues do not populate helical conformations on the NMR time scale in S46D as is evidenced by their large $^3J_{NH\alpha}$ couplings as well as fast exchange rates. If Leu53 and Gly54 were to assume a helical conformation in S46D, this would be reflected in downfield shifts of their amide protons, a change in the $^3J_{NH\alpha}$ coupling constant, increased protection of Leu53 and Gly54 amides, and stronger sequential and medium-range NOEs for these residues. None of these parameters change significantly in S46D compared to the native protein. Therefore, the difference in helix length in S46D crystal and NMR structures could be in part due to crystal packing effects or alternatively may be a reflection of the plasticity inherent in this region of the protein.

CONCLUSION

In conclusion, there are two important ramifications of the work described herein. *ec*HPr is currently the only protein in which the effect of N-capping on both local and global protein stability has been assessed. Our studies complement the previously reported results on T4 lysozyme and barnase. We find that, even for very short α-helices, N-capping residues can detectably affect helix stability in solution. Intriguingly, the increase in helix stability observed by hydrogen exchange is closely correlated to the increase in global stability measured by protein denaturation studies. Since the stabilization of secondary structure is a local event,

our data support the hierarchic or framework model for protein folding.

Secondly, even though *ec*HPr is not phosphorylated *in vivo* and cannot be phosphorylated *in vitro* at Ser46, *ec*S46D is a good functional analogue of P-Ser46 HPr (Napper et al., 1996). We have shown that the structural consequence of mutating Ser46 to an Asp in *ec*HPr is similar to that observed in P-Ser46 *bs*HPr (Pullen et al., 1995). Future studies will aim to understand how introduction of a phosphate or aspartic acid at the N-cap of helix B prevents interaction between HPr and other PTS proteins and why *ec*HPr is not phosphorylated by the ATP-dependent kinase.

ACKNOWLEDGMENT

We thank David Hyre for help with computer programming, George Wong for protein purification, and Bryan Jones and Peter Brzovic for critical reading of the manuscript.

REFERENCES

Archer, G. J., Ikura, M., Torchia, D. A., & Bax, A. (1991) *J. Magn. Reson. 95*, 636−641.
Bai, Y., Milne, J. S., Mayne, L., & Englander, W. S. (1993) *Proteins: Struct., Funct., Genet. 17*, 75−86.
Bai, Y., Milne, J., Mayne, L., & Englander, W. S. (1994) *Proteins: Struct., Funct., Genet. 20*, 4−14.
Bash, P. A., Pattabiraman, N., Hunag, C. C., Ferrin, T. E., & Langridge, R. (1983) *Science 222*, 1325−1327.
Becktel, W. J., & Schellman, J. A. (1987) *Biopolymers 11*, 1859−1877.
Bell, J. A., Becktel, W. J., Sauer, U., Baase, W. A., & Matthews, B. W. (1992) *Biochemistry 31*, 3590−3596.
Billeter, M., Neri, D., Otting, G., Qian, Y. Q., & Wüthrich, K. (1992) *J. Biomol. NMR 2*, 257−274.
Chakrabartty, A., & Baldwin, R. L. (1995) *Adv. Protein Chem. 46*, 141−176.
Chen, Y., Reizer, J., Saier, M. H., Jr., Fairbrother, W. J., & Wright, P. E. (1993) *Biochemistry 32*, 32−37.
Deutscher, J., & Saier, M. H., Jr. (1983) *Proc. Natl. Acad. Sci. U.S.A. 80*, 6790−6794.
Doig, A. J., & Baldwin, R. L. (1995) *Protein Sci. 4*, 1325−1336.
Doig, A. J., Chakrabartty, A., Klingler, T. M., & Baldwin, R. L. (1994) *Biochemistry 33*, 3396−3403.
Driscoll, P. C., Gronenborn, A. M., Wingfield, P. T., & Clore, G. M. (1990) *Biochemistry 29*, 4668−4682.
Ferrin, T. E., Huang, C. C., Jarvis, L. E., & Langridge, R. (1988) *J. Mol. Graphics 6*, 13−27.
Hammen, P. K., Waygood, E. B., & Klevit, R. E. (1991) *Biochemistry 30*, 11842−11850.
Herzberg, O., & Klevit, R. E. (1994) *Curr. Opin. Struct. Biol. 6*, 814−22.
Hoffman, R. C., Xu, R. X., Klevit, R. E., & Herriott J. R. (1993) *J. Magn. Reson. B 102*, 61−72.
Hol, W. G., van Duijnen, P. T., & Berendsen, H. J. (1978) *Nature 273*, 443−446.
Huang, C. C., Petterson, E. F., Klein, T. E., Ferrin, T. E., & Langride, R. (1991) *J. Mol. Graphics 9*, 230−236.
Hvidt, A., & Nielsen, S. O. (1966) *Adv. Protein Chem. 21*, 287−386.
Jia, Z., Quail, J. W., Waygood, E. B., & Delbaere, L. T. J. (1993) *J. Biol. Chem. 268*, 22490−22501.
Karplus, M. (1959) *J. Chem. Phys. 30*, 11−15.
Kraulis, P. L. (1991) *J. Appl. Crystallogr. 24*, 946−950.
Liao, D., & Herzberg, O. (1994) *Structure 2*, 1203−1216.
Loh, S. N., Prehoda, K. E., Wang, J., & Markley, J. L. (1994) *Tech. Protein Chem. 5*, 431−438.
Markley, J. (1975*) Acc. Chem. Res. 8*, 70−80.
Marion, D., & Wüthrich, K. (1983) *Biochem. Biophys. Res. Commun. 113*, 967−974.
Marion, D., Ikura, M., Tschudin, R., & Bax, A. (1989) *J. Magn. Reson. 85*, 397−399.
Mueller, L. (1987) *J. Magn. Reson. 72*, 191−197.
Napper, S., Anderson, J. W., Georges, F., Quail, J. W., Delbaere, L. T. J., & Waygood, E. B. (1996) *Biochemistry 35*, 11260−11267.
Neri, D., Otting, G., & Wüthrich, K. (1990) *J. Am. Chem. Soc. 112*, 3663−3665.
Nicholson, E. M., & Scholtz, J. M. (1996) *Biochemistry* (in press).
Nicholson, H., Becktel, W. J., & Matthews, B. W. (1988) *Nature 336*, 651−656.
Nicholson, H., Anderson, D. E., Dao-pin, S., & Matthews, B. W. (1991) *Biochemistry 30*, 9816−9828.
Norwood, T. J., Boyd, J., Heritage, J. E., Soffe, N., & Campbell, I. D. (1990) *J. Magn. Reson. 87*, 488−501.
Pace, C. N. (1986) *Methods Enzymol. 131*, 266−280.
Pardi, A., Billeter, M., & Wuthrich, K. (1984) *J. Mol. Biol. 180*, 741−151.
Presta, L. G., & Rose, G. D. (1988) *Science 240*, 1632−1641.
Pullen, K., Rajagopal, P., Branchini, B. R., Huffine, M. E., Reizer, J., Saier, M. H., Jr., Scholtz, J. M., & Klevit, R. E. (1995) *Protein Sci. 4*, 2478−2486.
Reizer, J., Sutrina, S. L., Saier, M. H., Jr., Stewart, G. C., Peterkofsky, A., & Reddy, P. (1989) *EMBO J. 8*, 2111−2120.
Richardson, J. S., & Richardson, D. C. (1988) *Science 240*, 1648−1652.
Roder, H. (1989) *Methods Enzymol. 176*, 446.
Scholtz, J. M. (1995) *Protein Sci. 4*, 35−43.
Scholtz, J. M., & Baldwin, R. L. (1992) *Ann. Rev. Biophys. Biomol. Struct. 21*, 95−118.
Serrano, L., & Fersht, A. R. (1989) *Nature 342*, 296−299.
Serrano, L., Sancho, J., Hershberg, M., Fersht, A. R. (1992) *J. Mol. Biol. 227*, 544−559.
Sharma, S., Georges, F., Delbaere, L. T. J., Lee, J. S., Klevit, R. E., & Waygood, E. B. (1991) *Proc. Natl. Acad. Sci. U.S.A. 88*, 4877−4881.
Spera, S., Ikura, M., & Bax, A. (1991) *J. Biomol. NMR 1*, 155−165.
States, D. J., Haberkorn, R. A., & Ruben, D. J. (1982) *J. Magn. Reson. 48*, 286.
van Nuland, N. A., Kroon, G. J., Dijkstra, K., Wolters, G. K., Scheek, R. M., & Robillard, G. T. (1993) *FEBS Lett. 3151*, 11−15.
van Nuland, N. A., Hangyi, I. W., van Schaik, R. C., Berendsen, J. C., van Gunsteren, W. F., Scheek, R. M., & Robillard, G. T. (1994) *J. Mol. Biol. 237*, 544−559.
van Nuland, N. A., Boelens, R., Scheek, R. M., & Robillard, G. T. (1995) *J. Mol. Biol. 246*, 180−93.
Wagner G. (1983) *Q. Rev. Biophys. 1*, 1−57.
Wagner, G., & Wüthrich, K. (1979) *J. Mol. Biol. 130*, 31.
Wand, A. J., Roder, H., & Englander, S. W. (1986) *Biochemistry 25*, 1107−1114.
Wittekind, M., Rajagopal, P., Branchini, B. R., Reizer, J., Saier, M. H., Jr., & Klevit, R. E. (1992) *Protein Sci. 1*, 1363−1376.
Wüthrich, K. (1986) *NMR of Proteins and Nucleic Acids*, John Wiley & Sons, Inc., New York, NY.

BI960349S